Theor Chem Acc (2010) 125:75–82
DOI 10.1007/s00214-009-0664-3

REGULAR ARTICLE

Dual-level direct dynamics studies on the reactions of tetramethylsilane with chlorine and bromine atoms

Hui Zhang · Gui-ling Zhang · Jing-yao Liu · Wen-jie Hou · Bo Liu · Ze-sheng Li

Received: 24 June 2009 / Accepted: 16 October 2009 / Published online: 5 November 2009

Abstract The multiple-channel reactions Cl + $Si(CH_3)_4$ and Br + $Si(CH_3)_4$ are investigated by direct dynamics method. The minimum energy path is calculated at the MP2/6-31+G(d,p) level, and energetic information is further refined by the MC-QCISD (single-point) method. The rate constants for individual reaction channel are calculated by the improved canonical variational transition state theory with small-curvature tunneling correction over the temperature range 200–3,000 K. The theoretical three-parameter expression $k_1(T) = 9.97 \times 10^{-13} T^{0.54} \exp(613.22/T)$ and $k_2(T) = 1.16 \times 10^{-17} T^{2.30} \exp(-3525.88/T)$ (in unit of cm^3 $molecule^{-1}$ s^{-1}) are given. Our calculations indicate that hydrogen abstraction channel is the major channel due to the smaller barrier height among feasible channels considered.

Keywords Gas-phase reaction · Transition state · Rate constants

Electronic supplementary material The online version of this article (doi:10.1007/s00214-009-0664-3) contains supplementary material, which is available to authorized users.

H. Zhang · G. Zhang · W. Hou · B. Liu (✉)
College of Chemical and Environmental Engineering, Harbin University of Science and Technology, 150080 Harbin, People's Republic of China
e-mail: hust_zhanghui1@hotmail.com

J. Liu
Institute of Theoretical Chemistry, State Key Laboratory of Theoretical and Computational Chemistry, Jilin University, 130023 Changchun, People's Republic of China

Z. Li
Department of Chemistry, Harbin Institute of Technology, Academy of Fundamental and Interdisciplinary Sciences, 150080 Harbin, People's Republic of China

1 Introduction

Silane and its methyl-substituted homolog are considered as important reagents in plasma chemical vapor deposition (CVD) and in the semiconductor manufacturing process. Tetramethylsilane is frequently used as a solvent. The use of volatile silicon compounds may lead to their emission into the atmosphere, where they can be removed by reactions with a variety of reactive species, such as hydroxyl, nitrate radicals, and halogen atoms. For most hydrocarbons, hydrogen abstraction by radicals is one of the major channels for their removal from the atmosphere [1, 2]. Hence, there is a particular need to investigate the chemistry of some methyl-substituted homolog reactions with Cl and Br. For the reactions Cl + $Si(CH_3)_4$ and Br + $Si(CH_3)_4$, the hydrogen atom can be abstracted, and the CH_3 group can also be abstracted; as a result, four reaction pathways are feasible, denoted as R1a, R1b, R2a, and R2b as follows:

$$Cl + Si(CH_3)_4 \rightarrow Si(CH_3)_3CH_2 + HCl \quad (R1a)$$
$$\rightarrow Si(CH_3)_3 + CH_3Cl \quad (R1b)$$
$$Br + Si(CH_3)_4 \rightarrow Si(CH_3)_3CH_2 + HBr \quad (R2a)$$
$$\rightarrow Si(CH_3)_3 + CH_3Br \quad (R2b)$$

CH_3-abstraction has not been reported in experiment and no theoretical works are related to the comparison of the reactivity between C–H bond and Si–C bond, but CH_3-abstraction channel is possible in principle. The present work aimed at determining whether CH_3-abstraction channel is available and could contribute to the whole reaction. There is very limited experimental literature concerning the title reactions. Thus, the rate constants of reaction OH + $Si(CH_3)_4$ and OH + $SiH(CH_3)_3$ calculated in the other paper [3] are added to discuss the reliability of

the calculated results on the rate constants of this class of hydrogen abstraction reactions. For the reaction OH + $Si(CH_3)_4$, the overall rate constants have been investigated by Goumri et al. [4], the expression $k = (1.2 \pm 0.2) \times 10^{-12}$ cm^3 $molecule^{-1}$ s^{-1} at 293–297 K. The rate constants, also obtained by Atkinson et al. [5] at 297 ± 2 K, by Sommerlade et al. [6] at 297 ± 2 K, and by Tuazon et al. [7] at 298 ± 2 K were $(1.00 \pm 0.27) \times 10^{-12}$, $(1.28 \pm 0.46) \times 10^{-12}$, and $(8.5 \pm 0.9) \times 10^{-13}$ (in unit of cm^3 $molecule^{-1}$ s^{-1}), respectively. The value of reaction OH + $Si(CH_3)_4$ taken from Goumri et al.'s work [4] is in good agreement with those values given by Atkinson et al. [5], Sommerlade et al. [6], and Tuazon et al. [7] at room temperature.

Because measurements were done mostly at the lower temperature range of the title reactions, theoretical investigation is desirable to give a further understanding of the mechanism of those multiple-channel reactions and to evaluate the rate constants at high temperatures. To the best of our knowledge, the rate constants of the title reactions have not been studied theoretically.

In this paper, dual-level direct dynamics method [8–12] is employed to study the kinetics of the $Si(CH_3)_4$ reactions with Cl and Br atoms. The potential energy surface information, including geometries, energies, gradients, force constants of all the stationary points (reactant, products, complexes, and transition states), and some extra points along the minimum energy path (MEP), is obtained directly from electronic structure calculations. Single-point energies are calculated by the MC-QCISD method [13]. Subsequently, by means of the POLYRATE 9.1 program [14], the rate constants of these reaction channels are calculated by the variational transition state theory (VTST) [15, 16] proposed by Truhlar and coworkers. The comparison between the theoretical and experimental results is discussed. Our results may be helpful for further experimental investigations.

2 Computational method

In the present work, the equilibrium geometries and frequencies of all the stationary points (reactant, products, complexes, and transition states) are optimized at the restricted or unrestricted second-order Møller–Plesset perturbation (MP2) [17–19] level with the 6-31+G(d,p) basis set. The MEP is obtained by intrinsic reaction coordinate (IRC) theory with a gradient step-size of 0.05 $(amu)^{1/2}$ bohr. Then, the first and second energy derivatives are obtained to calculate the curvature of the reaction path and the generalized vibrational frequencies along the reaction path. In order to obtain more accurate energies and barrier heights, the energies are calculated by the MC-QCISD method (multi-coefficient correlation method based on quadratic configuration interaction with single and double excitations proposed by Fast and Truhlar) [13] based on the MP2/6-31+G(d,p) geometries. All the electronic structure calculations are performed by the GAUSSIAN03 program package [20].

VTST [15, 16] is employed to calculate the rate constants by the POLYRATE 9.1 program [14]. The theoretical rate constants for each reaction channel over the temperature range 200–3,000 K are calculated by the improved canonical variational transition state theory (ICVT) [21] incorporating small-curvature tunneling (SCT) [22, 23] contributions proposed by Truhlar and coworkers [21]. For the title reaction, most of the vibrational modes are treated as quantum–mechanical separable harmonic oscillators except for the lowest modes. The hindered-rotor approximation of Truhlar and Chuang [24, 25] is used for calculating the partition function of the four vibrational modes. The curvature components are calculated by using a quadratic fit to obtain the derivative of the gradient with respect to the reaction coordinate. Since $Si(CH_3)_4$ is Td symmetry, the symmetry factor $\sigma = 12$ for the reaction channels R1a, R1b, R2a, and R2b are taken into account in the rate constants calculation. The total rate constants k are calculated from the sum of the individual rate constants, i.e., $k_1 = k_{1a} + k_{1b}$, and $k_2 = k_{2a} + k_{2b}$.

3 Results and discussion

3.1 Stationary points

The optimized geometries of the reactant ($Si(CH_3)_4$), products ($Si(CH_3)_3CH_2$, $Si(CH_3)_3$, CH_3Cl, CH_3Br, HCl, and HBr), complexes (R1aR and R2aF), and transition states (TS1a, TS1b, TS2a, and TS2b) calculated at the MP2/6-31+G(d,p) level are presented in Fig. 1, along with the available experimental values [26, 27]. The theoretical geometric parameters of CH_3Cl, CH_3Br, HCl, and HBr are in good agreement with the corresponding experimental values [26, 27]. Furthermore, a hydrogen-bonded complex (R1aR) is presented on the reactant side for reaction R1a. At the MP2 level, the distance between the hydrogen atom in CH_3 group of $Si(CH_3)_4$ and the chlorine atom in R1aR is 3.498 Å, while the other bond lengths are very close to those of the reactant. On the product side of reaction R2a, there is one complex (R2aF), the distance between the carbon atom in CH_3 group of $Si(CH_3)_4$ and the hydrogen atom of the HBr in R2aF is 2.206 Å, while the other bond lengths are very close to those of the products. Figure 1 shows that the transition state TS1a, TS1b, TS2a, and TS2b have the same symmetry, C_1. Product $Si(CH_3)_3CH_2$ also has symmetry C_1; when symmetry is restricted to C_S, the corresponding frequencies have three imaginary

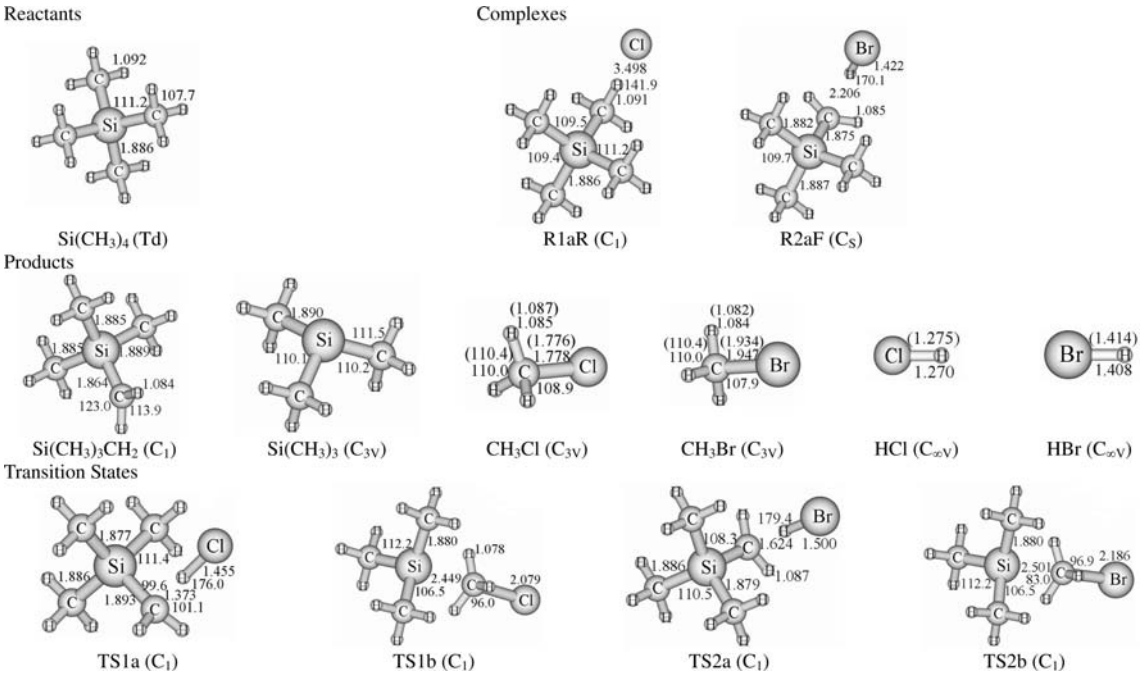

Fig. 1 Optimized geometries of the reactant, products, and transition states at the MP2/6-31+G(d,p) level. The values in *parentheses* are the experimental values (Ref. [26] for CH_3Cl and CH_3Br, and Ref. [27] for HCl and HBr). Bond lengths are in *angstrom* and angles are in *degree*

frequencies at the same level. In TS1a, TS1b, TS2a, and TS2b structures, the breaking bonds C–H and Si–C increase by 26, 30, 49, and 33% compared to the equilibrium bond length in $Si(CH_3)_4$; the forming bonds H–Cl, C–Cl, H–Br, and C–Br stretch by 15, 17, 7, and 12% over the equilibrium bond lengths in isolated HCl, CH_3Cl, HBr, and CH_3Br, respectively. The elongation of the breaking bond is larger than that of the forming bond, indicating that TS1a, TS1b, TS2a, and TS2b of the title reactions are all product-like, i.e., all the four reaction channels will proceed via "late" transition states.

Table S1 as supporting information lists the harmonic vibrational frequencies of the reactant, products, complexes, and transition states calculated at the MP2/6-31+G(d,p) level as well as the available experimental values [28–31]. For the species $Si(CH_3)_4$, CH_3Cl, CH_3Br, HCl, and HBr, the calculated frequencies are in good agreement with the experimental values. The four transition states are all confirmed by normal-mode analysis to have one imaginary frequency, which corresponds to the stretching modes of coupling between breaking and forming bonds. The values of those imaginary frequencies are $1{,}120i$ cm^{-1} for TS1a, $708i$ cm^{-1} for TS1b, $302i$ cm^{-1} for TS2a, and $642i$ cm^{-1} for TS2b.

3.2 Energetics

The reaction enthalpies (ΔH^0_{298}) and potential barrier heights (ΔE^{TS}) with zero-point energy (ZPE) corrections for R1a, R1b, R2a, and R2b reaction channels calculated at the MC-QCISD//MP2/6-31+G(d,p) level are listed in Table 1. It is shown that the three individual reactions R1b, R2a, and R2b are all endothermic reaction, which is consistent with the discussion of Hammond's postulate [32]. For the reaction channels R1b and R2b, the calculated values (9.60 and 20.18 kcal/mol) are quite different from that of the experimental ones (23.56 ± 1.67 and 37.61 ± 1.86 kcal/mol), which were derived from the experimental standard heats of formation (Cl, 28.97 kcal/mol [31]; Br, 26.72 kcal/mol [31]; $Si(CH_3)_4$, −68.45 kcal/mol [31]; $Si(CH_3)_3$, 4.07 ± 1.67 kcal/mol [33]; CH_3Cl, −19.99 kcal/mol [31]; CH_3Br, −8.19 ± 0.19 kcal/mol [34]). This large difference is surprising, since MC-QCISD has been successfully applied in our previous studies [35, 36] as well as in others' studies [37]. To further test the reliability of this method, we chose two similar systems, OH + $SiH(CH_3)_3$ and OH + $Si(CH_3)_4$, as target reactions and redid the reaction enthalpies and potential energy barriers at the MC-QCISD level, since they were studied previously [38] at the BMC-CCSD [39] level (a new multi-coefficient correlation method based on the coupled cluster theory with single and double excitations) and obtained good agreement with the experimental data [31, 33, 40]. The calculated reaction enthalpies, −27.05 and –26.31 kcal/mol, are in good agreement with the corresponding experimental value (−24.11 ± 2.63), which was derived from the standard heats of formation ($Si(CH_3)_3$, 4.07 ± 1.67 kcal/mol [33]; OH, 9.33 kcal/mol [31]; $SiH(CH_3)_3$,

Table 1 The reaction enthalpies at 298 K (ΔH^0_{298}), the barrier heights TSs (ΔE^{TS}) (kcal/mol) with zero-point energy (ZPE) correction for the title reactions at the MC-QCISD//MP2/6-31+G(d,p) level together with the experimental values

	MC-QCISD//MP2/6-31+G(d,p)	BMC-CCSD//MP2/6-311+G(2d,2p)	Expt.
ΔH^0_{298}			
$Cl + Si(CH_3)_4 \rightarrow Si(CH_3)_3CH_2 + HCl$ (R1a)	−3.19		
$Cl + Si(CH_3)_4 \rightarrow Si(CH_3)_3 + CH_3Cl$ (R1b)	9.60		23.56 ± 1.67
$Br + Si(CH_3)_4 \rightarrow Si(CH_3)_3CH_2 + HBr$ (R2a)	10.54		
$Br + Si(CH_3)_4 \rightarrow Si(CH_3)_3 + CH_3Br$ (R2b)	20.18		37.61 ± 1.86
$OH + Si(CH_3)_4 \rightarrow Si(CH_3)_3CH_2 + H_2O$ (R3)	−19.34	−18.62	
$OH + SiH(CH_3)_3 \rightarrow Si(CH_3)_3 + H_2O$	−27.05	−26.31	−24.11 ± 2.63
ΔE^{TS} + ZPE			
$Cl + Si(CH_3)_4 \rightarrow Si(CH_3)_3CH_2 + HCl$ (R1a)	−3.34		
$Cl + Si(CH_3)_4 \rightarrow Si(CH_3)_3 + CH_3Cl$ (R1b)	22.70		
$Br + Si(CH_3)_4 \rightarrow Si(CH_3)_3CH_2 + HBr$ (R2a)	7.33		
$Br + Si(CH_3)_4 \rightarrow Si(CH_3)_3 + CH_3Br$ (R2b)	29.79		
$OH + Si(CH_3)_4 \rightarrow Si(CH_3)_3CH_2 + H_2O$ (R3)	1.71	0.35	
$OH + SiH(CH_3)_3 \rightarrow Si(CH_3)_3 + H_2O$	−1.89	−2.48	

Experimental value derived from the standard heats of formation (in kcal/mol) of species involved in the reactions: Cl, 28.97 kcal/mol [31]; Br, 26.72 kcal/mol [31]; $Si(CH_3)_4$, −68.45 kcal/mol [31]; $Si(CH_3)_3$, 4.07 ± 1.67 kcal/mol [33]; CH_3Cl, −19.99 kcal/mol [31]; CH_3Br, −8.19 ± 0.19 kcal/mol [34]; OH, 9.33 kcal/mol [31]; $SiH(CH_3)_3$, −39.00 ± 0.96 kcal/mol [40]; H_2O, −57.85 kcal/mol [31]

−39.00 ± 0.96 kcal/mol [40]; H_2O, −57.85 kcal/mol [31]). The corresponding values are also listed in Table 1. It is seen that for these two reactions, the agreement between the results at the two levels and between the theoretical and the available experimental value is good. The agreement between the MC-QCISD and BMC-CCSD is reasonable, while the larger discrepancy indicates that our results may not be quantitatively reliable.

The schematic potential energy surfaces of the title reactions obtained at the MC-QCISD//MP2/6-31+G(d,p)+ZPE level are plotted in Fig. 2. Note that the energy of reactant is set to zero for reference. The values in parentheses are calculated at the MP2/6-31+G(d,p) level and include the ZPE corrections. For reaction R1a, the complex R1aR is about 3.59 kcal/mol lower than that of the corresponding reactants at the MC-QCISD//MP2/6-31+G(d,p)+ZPE level. And for reaction R2a, the complex R2aF with the energy of 2.56 kcal/mol lower than that of the corresponding products at the same level. For reaction R1, the barrier of TS1a taking the value of −3.34 kcal/mol at the same level is about 26.0 kcal/mol lower than that of TS1b, which indicates that H-abstraction channel (TS1a) is more favorable than the CH_3-abstraction channel (TS1b). At the same time, reaction R1a is more exothermic than reaction R1b by about 13.71 kcal/mol. On the basis of above calculation, reaction R1a is more favorable than reaction R1b both thermodynamically and kinetically and will dominate the reaction, while the CH_3-abstraction channel may be negligible. Similarly, for reaction $Si(CH_3)_4$ with Br atom, the potential barrier heights are 7.33 kcal/mol

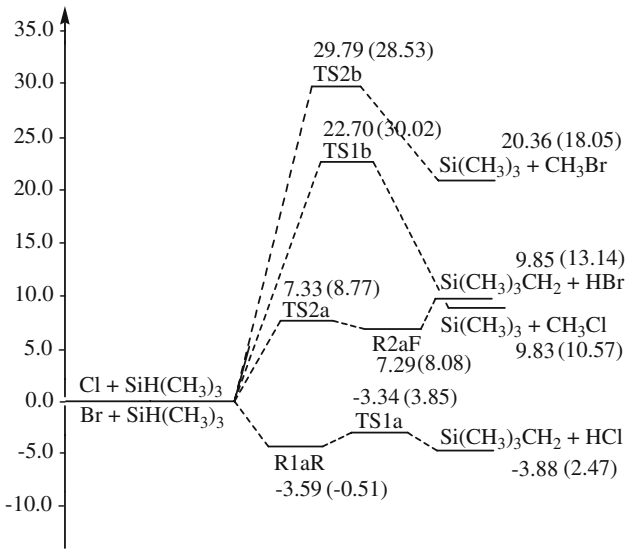

Fig. 2 Schematic potential energy surface for the title reaction system. Relative energies are calculated at the MC-QCISD//MP2/6-31+G(d,p) level including ZPE correction in (kcal/mol). The values in *parentheses* are calculated at the MP2/6-31+G(d,p) level including ZPE correction in (kcal/mol)

for reaction R2a and 29.79 kcal/mol for reaction R2b at MC-QCISD//MP2/6-31+G(d,p)+ZPE level, and the value of reaction enthalpies with ZPE corrections is 9.85 for reaction channel R2a is lower than that of R2b by about 10.5 kcal/mol. So reaction channel R2a is also more favorable than reaction channel R2b both thermodynamically and kinetically. H-abstraction channel (R2a) is

Table 2 Calculated TST, ICVT, and ICVT/SCT rate constants (cm^3 $molecule^{-1}$ s^{-1}) of the reaction channels R1a, k_{1a}, R1b, k_{1b}, and overall rate constants, k_1, in the temperature region 200–3,000 K at the MC-QCISD//MP2/6-31+G(d,p) level

T(K)	k_{1a}			k_{1b}			k_1
	TST	ICVT	ICVT/SCT	TST	ICVT	ICVT/SCT	ICVT/SCT
200	5.29×10^{-8}	3.35×10^{-10}	3.44×10^{-10}	9.06×10^{-36}	8.53×10^{-36}	3.97×10^{-35}	3.44×10^{-10}
225	2.34×10^{-8}	2.76×10^{-10}	2.82×10^{-10}	6.39×10^{-33}	6.19×10^{-33}	2.02×10^{-32}	2.82×10^{-10}
250	1.24×10^{-8}	2.31×10^{-10}	2.35×10^{-10}	1.24×10^{-30}	1.23×10^{-30}	3.12×10^{-30}	2.35×10^{-10}
298	5.16×10^{-9}	1.76×10^{-10}	1.79×10^{-10}	2.67×10^{-27}	2.74×10^{-27}	5.09×10^{-27}	1.79×10^{-10}
350	2.73×10^{-9}	1.43×10^{-10}	1.44×10^{-10}	1.06×10^{-24}	1.11×10^{-24}	1.69×10^{-24}	1.44×10^{-10}
400	1.79×10^{-9}	1.24×10^{-10}	1.24×10^{-10}	7.86×10^{-23}	8.36×10^{-23}	1.13×10^{-22}	1.24×10^{-10}
450	1.33×10^{-9}	1.11×10^{-10}	1.11×10^{-10}	2.28×10^{-21}	2.48×10^{-21}	3.05×10^{-21}	1.11×10^{-10}
500	1.07×10^{-9}	1.02×10^{-10}	1.02×10^{-10}	3.42×10^{-20}	3.73×10^{-20}	4.35×10^{-20}	1.02×10^{-10}
600	8.15×10^{-10}	9.00×10^{-11}	9.03×10^{-11}	2.06×10^{-18}	2.22×10^{-18}	2.43×10^{-18}	9.03×10^{-11}
700	7.04×10^{-10}	8.30×10^{-11}	8.32×10^{-11}	3.96×10^{-17}	4.24×10^{-17}	4.46×10^{-17}	8.32×10^{-11}
800	6.55×10^{-10}	7.85×10^{-11}	7.87×10^{-11}	3.72×10^{-16}	3.96×10^{-16}	4.06×10^{-16}	7.87×10^{-11}
900	6.36×10^{-10}	7.56×10^{-11}	7.57×10^{-11}	2.15×10^{-15}	2.28×10^{-15}	2.31×10^{-15}	7.57×10^{-11}
1,000	6.36×10^{-10}	7.37×10^{-11}	7.38×10^{-11}	8.88×10^{-15}	9.42×10^{-15}	9.42×10^{-15}	7.38×10^{-11}
1,200	6.63×10^{-10}	7.18×10^{-11}	7.18×10^{-11}	7.71×10^{-14}	8.56×10^{-14}	7.99×10^{-14}	7.19×10^{-11}
1,500	7.43×10^{-10}	7.16×10^{-11}	7.17×10^{-11}	7.02×10^{-13}	7.96×10^{-13}	7.02×10^{-13}	7.24×10^{-11}
2,000	9.20×10^{-10}	7.49×10^{-11}	7.49×10^{-11}	6.99×10^{-12}	7.72×10^{-12}	6.67×10^{-12}	8.16×10^{-11}
2,400	1.08×10^{-9}	7.90×10^{-11}	7.90×10^{-11}	2.32×10^{-11}	2.50×10^{-11}	2.16×10^{-11}	1.01×10^{-10}
3,000	1.34×10^{-9}	8.63×10^{-11}	8.63×10^{-11}	8.16×10^{-11}	8.38×10^{-11}	7.35×10^{-11}	1.60×10^{-10}

expected to be the major one with larger rate constants, and the CH_3-abstraction channel is a minor pathway.

3.3 Rate constants

Dual-level direct dynamics calculations [8–12] of the title reactions are carried out at the MC-QCISD//MP2/6-31+G(d,p) level. The rate constants of the individual channel, k_{1a}, k_{1b}, k_{2a}, k_{2b}, and overall rate constants, k_1 and k_2, are evaluated by conventional transition state theory (TST), the ICVT, and the ICVT with the SCT contributions in a wide temperature range from 200 to 3,000 K. In the other paper [3], the rate constants of reaction OH + $Si(CH_3)_4$ have been calculated at BMC-CCSD//MP2/6-311+G(2d,2p) level; the theoretical CVT/SCT rate constant is in good agreement with the available experimental values [4–7], and the ratio of $k_{CVT/SCT}$/kexptl remains within a factor of approximately 0.65–0.97 at the room temperature. In the present work, the reactivity trend of different halogen (Cl and Br) reaction with tetramethylsilane on the rate constants will be discussed. We hope that the present calculations may provide reliable estimations of the rate constants for the reactions Cl + $Si(CH_3)_4$ and Br + $Si(CH_3)_4$ over a wide temperature range. The TST, ICVT, ICVT/SCT rate constants of the four reaction channels and overall rate constants for R1 and R2 are given in Tables 2 and 3 and Fig. 3, respectively. The anti-Arrhenius behavior of k_1 could be clearly seen from the auxiliary small figure in Fig. 3. Tables 2 and 3 show that the variational effect of R1a, i.e., the ratio between TST and ICVT rate constants, plays an important role at the lower temperatures and is not significant at high temperatures. For example, the ratios of k_{1a}(TST)/k_{1a}(ICVT) are 20.04, 5.93, and 4.31 at 200, 400, and 600 K, respectively, while the variational effect of the other three reaction channels is almost negligible. The existence of a significant variational effect on the rate of R1a, which is not seen in the other three reactions that were studied, likely reflects the presence of the entrance channel complex in R1a. This is in line with the potential energy surfaces results calculated earlier. And the ICVT/SCT and ICVT rate constants of the four reaction channels are nearly the same in the whole temperature region, which indicates that the tunneling effect is almost negligible.

From the Tables can also be found that the values of k_{1a} and k_{2a} are much larger than those of k_{1b} and k_{2b} by about 1–26, and 1–23 orders of magnitude in the temperature range 200–3,000 K and the total rate constants are almost equal to reactions R1a and R2a, respectively. Thus, on the basis of our calculation the hydrogen abstraction channel R1a and R2a are the major reaction channels over the entire temperature range, while the other two reaction channels R1b and R2b are always minor pathways over the temperature range 200–3,000 K. This is in line with the calculated potential energy barrier heights and the reaction enthalpies results mentioned earlier.

Table 3 Calculated TST, ICVT, and ICVT/SCT rate constants (cm^3 $molecule^{-1}$ s^{-1}) of the four reaction channels R2a, k_{2a}, R2b, k_{2b}, and overall rate constants, k_2, in the temperature region 200–3,000 K at the MC-QCISD//MP2/6-31+G(d,p) level

T(K)	k_{2a}			k_{2b}			k_2
	TST	ICVT	ICVT/SCT	TST	ICVT	ICVT/SCT	ICVT/SCT
200	8.83×10^{-20}	5.08×10^{-20}	5.08×10^{-20}	9.78×10^{-44}	9.77×10^{-44}	3.58×10^{-43}	5.08×10^{-20}
225	7.57×10^{-19}	4.74×10^{-19}	4.74×10^{-19}	5.34×10^{-40}	5.50×10^{-40}	1.48×10^{-39}	4.74×10^{-19}
250	4.31×10^{-18}	2.89×10^{-18}	2.89×10^{-18}	5.34×10^{-37}	5.61×10^{-37}	1.23×10^{-36}	2.89×10^{-18}
298	5.61×10^{-17}	4.17×10^{-17}	4.17×10^{-17}	1.25×10^{-32}	1.35×10^{-32}	2.26×10^{-32}	4.17×10^{-17}
350	4.32×10^{-16}	3.49×10^{-16}	3.49×10^{-16}	3.15×10^{-29}	3.52×10^{-29}	4.86×10^{-29}	3.49×10^{-16}
400	1.95×10^{-15}	1.67×10^{-15}	1.67×10^{-15}	8.91×10^{-27}	9.78×10^{-27}	1.24×10^{-26}	1.67×10^{-15}
450	6.53×10^{-15}	5.83×10^{-15}	5.83×10^{-15}	7.35×10^{-25}	8.05×10^{-25}	9.56×10^{-25}	5.83×10^{-15}
500	1.77×10^{-14}	1.63×10^{-14}	1.63×10^{-14}	2.57×10^{-23}	2.78×10^{-23}	3.17×10^{-23}	1.63×10^{-14}
600	8.40×10^{-14}	8.02×10^{-14}	8.02×10^{-14}	5.52×10^{-21}	5.90×10^{-21}	6.39×10^{-21}	8.02×10^{-14}
700	2.73×10^{-13}	2.65×10^{-13}	2.65×10^{-13}	2.66×10^{-19}	2.83×10^{-19}	2.96×10^{-19}	2.65×10^{-13}
800	6.92×10^{-13}	6.79×10^{-13}	6.79×10^{-13}	5.01×10^{-18}	5.32×10^{-18}	5.45×10^{-18}	6.79×10^{-13}
900	1.48×10^{-12}	1.46×10^{-12}	1.46×10^{-12}	5.01×10^{-17}	5.30×10^{-17}	5.36×10^{-17}	1.46×10^{-12}
1,000	2.79×10^{-12}	2.77×10^{-12}	2.77×10^{-12}	3.24×10^{-16}	3.42×10^{-16}	3.42×10^{-16}	2.77×10^{-12}
1,200	7.68×10^{-12}	7.65×10^{-12}	7.65×10^{-12}	5.49×10^{-15}	5.73×10^{-15}	5.67×10^{-15}	7.66×10^{-12}
1,500	2.31×10^{-11}	2.31×10^{-11}	2.31×10^{-11}	9.87×10^{-14}	1.15×10^{-13}	9.95×10^{-14}	2.32×10^{-11}
2,000	7.95×10^{-11}	7.95×10^{-11}	7.95×10^{-11}	1.96×10^{-12}	2.40×10^{-12}	1.85×10^{-12}	8.13×10^{-11}
2,400	1.58×10^{-10}	1.58×10^{-10}	1.58×10^{-10}	9.21×10^{-12}	1.08×10^{-11}	8.25×10^{-12}	1.66×10^{-10}
3,000	3.39×10^{-10}	3.39×10^{-10}	3.39×10^{-10}	4.59×10^{-11}	7.40×10^{-11}	3.89×10^{-11}	3.78×10^{-10}

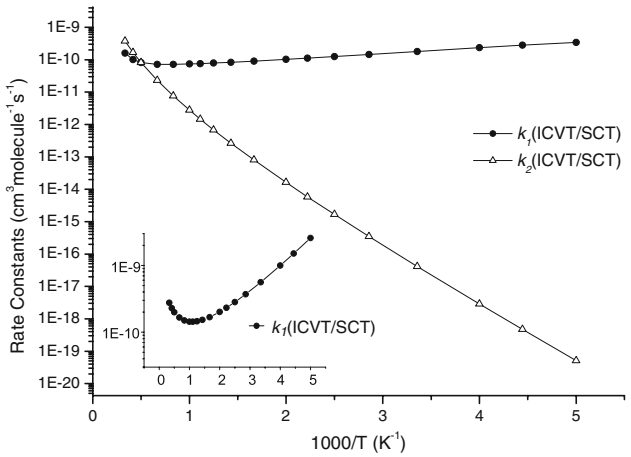

Fig. 3 The ICVT/SCT rate constants calculated at the MC-QCISD//MP2/6-31+G(d,p) level for the title reactions, R1 (k_1) and R2 (k_2) (in cm^3 $molecule^{-1}$ s^{-1}), versus 1,000/T between 200 and 3,000 K

We hope that our present study may provide useful information for future laboratory investigations. For convenience of future experimental measurements, the three-parameter fits of the ICVT/SCT rate constants of four reaction channels, and the whole reaction in the temperature range from 200 to 3,000 K are performed and the expressions are given as follows (in unit of cm^3 $molecule^{-1}$ s^{-1}):

$$k_{1a}(T) = 2.83 \times 10^{-12} T^{0.40} \exp(552.25/T)$$

$$k_{1b}(T) = 4.57 \times 10^{-15} T^{1.55} \exp(-11126.09/T)$$

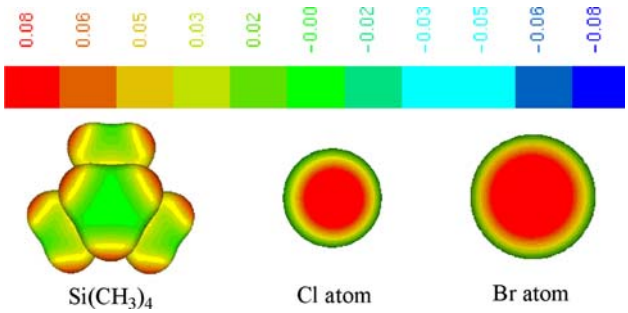

Fig. 4 Calculated electrostatic potential textured Van der Waals surfaces for the reactants

$$k_{2a}(T) = 1.37 \times 10^{-17} T^{2.28} \exp(-3535.72/T)$$

$$k_{2b}(T) = 1.16 \times 10^{-15} T^{1.80} \exp(-14821.71/T)$$

$$k_1(T) = 9.97 \times 10^{-13} T^{0.54} \exp(613.22/T)$$

$$k_2(T) = 1.16 \times 10^{-17} T^{2.30} \exp(-3525.88/T).$$

3.4 Reactivity trends

The molecular electrostatic potential is an important tool to analyze molecular reactivity because it can provide the information about local polarity. Figure 4 gives the distribution of the molecular electrostatic potential. There, the most negative and positive potentials are assigned to be blue and red, respectively, and the color spectrum is

mapped to all other values by linear interpolation. The more positive potential region (more red) will be more favored for the Cl or Br to attack at. It is found that in molecule $Si(CH_3)_4$ the H atoms bear stronger positive potential (red) than the C atoms of CH_3 groups (green), indicating that the H atoms can be more easily attacked by Cl or Br. It is found that in molecule $Si(CH_3)_4$ the H atoms bear stronger positive potential (red) than the C atoms of CH_3 groups (green), indicating that the H atoms can be more easily attacked by the nucleophiles. Note that the halogen atom is encircled by marked negative potential; therefore, the halogen atom is more preferable for attacking the H atom of $Si(CH_3)_4$ compared to the CH_3 group. From these results we could infer that the H-abstraction reaction channel of $Si(CH_3)_4$ with halogen (Cl and Br) could occur more easily than the CH_3-abstraction reaction. This is in line with the rate constant results calculated above.

4 Conclusion

In this paper, the multi-channel reactions of $Si(CH_3)_4$ with Cl and Br atoms are studied by a dual-level direct dynamics method. The potential energy surface information is obtained at the MP2/6-31+G(d,p) level, and energies of the stationary points and a few extra points along the MEP are refined at the MC-QCISD level. For the title reactions, four reaction channels are identified; hydrogen abstraction reaction channels are the major pathways. The rate constants for four reaction channels are calculated by the ICVT incorporating SCT contribution at the MC-QCISD//MP2 level. The calculated results show that the variational effect plays an important role in the calculation of rate constants for R1a reaction channel at the lower temperatures. The three-parameter rate-temperature formulae for the reactions $Cl + Si(CH_3)_4$ and $Br + Si(CH_3)_4$ in the temperature range 200 to 3,000 K are fitted and given as follows (in cm^3 $molecule^{-1}$ s^{-1}):

$$k_1(T) = 9.97 \times 10^{-13} T^{0.54} \exp(613.22/T)$$

$$k_2(T) = 1.16 \times 10^{-17} T^{2.30} \exp(-3525.88/T).$$

Acknowledgments The authors thank Professor Donald G. Truhlar for providing POLYRATE 9.1 program. This work is supported by the National Natural Science Foundation of China (20333050, 20303007, 50743013, and 20973049), the Program for New Century Excellent Talents in University (NCET), the Key subject of Science and Technology by the Ministry of Education of China, the Key subject of Science and Technology by Jilin Province, the Foundation for University Key Teacher by the Department of Education of Heilongjiang Province (1152G010), the SF of Graduate Innovation by Department of Education of Heilongjiang province (YJSCX2009-055HLJ), the SF for Postdoctoral of HLJ province (LBH-Q07058), and Natural Science Foundation of Heilongjiang Province (B200605).

References

1. Calvert JG, Atkinson R, Kerr JA, Madronich S, Moortgat GK, Wallington TJ, Yarwood G (2000) The mechanisms of atmospheric oxidation of the alkenes. Oxford, New York
2. Calvert JG, Atkinson R, Becker KH, Kamens RH, Seinfeld JH, Wallington TJ, Yarwood G (2002) The mechanisms of atmospheric oxidation of the aromatic hydrocarbons. Oxford, New York
3. Zhang H, Zhang GL, Wang Y, Yu XY, Liu B, Liu JY, Li ZS (2008) Theo Chem Acc 119:319
4. Goumri A, Yuan J, Hommel EL, Marshall P (2003) Chem Phys Lett 375:149
5. Atkinson R (1991) Environ Sci Technol 25:863
6. Sommerlade R, Parlar H, Wrobel D, Kochs P (1993) Environ Sci Technol 27:2435
7. Tuazon EC, Aschmann SM, Atkinson R (2000) Environ Sci Technol 34:1970
8. Bell RL, Truong TN (1994) J Chem Phys 101:10442
9. Truong TN, Duncan WT, Bell RL (1996) Chemical applications of density functional theory. American Chemical Society, Washington, DC, p 85
10. Truhlar DG (1995) In: Heidrich D (ed) The reaction path in chemistry: current approaches and perspectives. Kluwer, Dordrecht, The Netherlands, p 229
11. Corchado JC, Espinosa-Garcia J, Hu W-P, Rossi I, Truhlar DG (1995) J Phys Chem 99:687
12. Hu W-P, Truhlar DG (1996) J Am Chem Soc 118:860
13. Fast PL, Truhlar DG (2000) J Phys Chem A 104:6111
14. Corchado JC, Chuang Y-Y, Fast PL, Villa J, Hu W-P, Liu Y-P, Lynch GC, Nguyen KA, Jackels CF, Melissas VS, Lynch BJ, Rossi I, Coitino EL, Ramos AF, Pu J, Albu TV (2002) POLYRATE version 9.1. Department of Chemistry and Supercomputer Institute, University of Minnesota, Minneapolis, Minnesota
15. Truhlar DG, Garrett BC (1980) Acc Chem Res 13:440
16. Truhlar DG, Isaacson AD, Garrett BC (1985) Generalized transition state theory. In: Baer M (ed) The theory of chemical reaction dynamics, vol 4. CRC Press, Boca Raton, FL, p 65
17. Duncan WT, Truong TN (1995) J Chem Phys 103:9642
18. Frisch MJ, Head-Gordon M, Pople JA (1990) Chem Phys Lett 166:275
19. Head-Gordon M, Pople JA, Frisch MJ (1988) Chem Phys Lett 153:503
20. Frisch MJ, Trucks GW, Schlegel HB, Scuseria GE, Robb MA, Cheeseman JR, Montgomery JA Jr, Vreven T, Kudin KN, Burant JC, Millam JM, Iyengar SS, Tomasi J, Barone V, Mennucci B, Cossi M, Scalmani G, Rega N, Petersson GA, Nakatsuji H, Hada M, Ehara M, Toyota K, Fukuda R, Hasegawa J, Ishida M, Nakajima T, Honda Y, Kitao O, Nakai H, Klene M, Li X, Knox JE, Hratchian HP, Cross JB, Adamo C, Jaramillo J, Gomperts R, Stratmann RE, Yazyev O, Austin AJ, Cammi R, Pomelli C, Ochterski JW, Ayala PY, Morokuma K, Voth GA, Salvador P, Dannenberg JJ, Zakrzewski VG, Dapprich S, Daniels AD, Strain MC, Farkas O, Malick DK, Rabuck AD, Raghavachari K, Foresman JB, Ortiz JV, Cui Q, Baboul AG, Clifford S, Cioslowski J, Stefanov BB, Liu G, Liashenko A, Piskorz P, Komaromi I, Martin RL, Fox DJ, Keith T, Al-Laham MA, Peng CY, Nanayakkara A, Challacombe M, Gill PMW, Johnson B, Chen W, Wong MW, Gonzalez C, Pople JA (2003) Gaussian, Inc., Pittsburgh, PA
21. Garrett BC, Truhlar DG, Grev RS, Magnuson AW (1980) J Phys Chem 84:1730
22. Lu DH, Truong TN, Melissas VS, Lynch GC, Liu YP, Grarrett BC, Steckler R, Issacson AD, Rai SN, Hancock GC, Lauderdale JG, Joseph T, Truhlar DG (1992) Comput Phys Commun 71:235

23. Liu Y-P, Lynch GC, Truong TN, Lu D-H, Truhlar DG, Garrett BC (1993) J Am Chem Soc 115:2408
24. Truhlar DG (1991) J Comput Chem 12:266
25. Chuang YY, Truhlar DG (2000) J Chem Phys 112:1221
26. Kuchitsu K (1998) In: Structure of free polyatomic molecules basic data, vol 1. Springer, Berlin, p 104
27. NIST Chemistry WebBook, NIST Standard Reference Database Number 69, June 2005 Release, Data compiled by K. P. Huber and G. Herzberg
28. In NIST Chemistry WebBook, NIST Standard Reference Database Number 69, June 2005 Release, Vibrational frequency date compiled by Coblentz Society, Inc
29. In NIST Chemistry WebBook, NIST Standard Reference Database Number 69, June 2005 Release, Vibrational frequency date compiled by T. Shimanouchi
30. Chase MW Jr, Davies CA, Downey JR, Fryrip DJ, McDonald RA, Syverud AN (1985) JANAF thermochemical tables. Ref Data 14(Suppl 1):1
31. Chase MW (1998) NIST-JANAF themochemical tables. J Phys Chem Ref Data Monograph 9:1–1951
32. Hammond GS (1955) J Am Chem Soc 77:334
33. Ding L, Marshall P (1992) J Am Chem Soc 114:5754
34. Ferguson KC, Okafo EN, Whittle E (1973) J Chem Soc Faraday Trans 1(69):295
35. Zhang H, Zhang GL, Liu JY, Miao S, Liu B, Li ZS (2009) J Comput Chem 30:236
36. Zhang H, Zhang GL, Liu JY, Liu CY, Liu B, Li ZS (2009) Theor Chem Acc 122:107
37. Phillips JA, Cramer CJ (2007) J Phys Chem B 111:1408
38. Zhang H, Zhang GL, Wang Y, Yu XY, Liu B, Liu JY, Li ZS (2008) Theor Chem Acc 119:319
39. Lynch BJ, Zhao Y, Truhlar DG (2005) J Phys Chem A 109:1643
40. Walsh R (1992) In: Martinho Simões JA (ed) Energetica of organometallic species; NATO-ASI Series C, 367. Kluwer, Dordrecht (Chap 11)